

Effects of spin and exchange interaction on the Coulomb-blockade peak statistics in quantum dots

Y. Alhassid and T. Rupp
*Center for Theoretical Physics, Sloane Physics Laboratory,
 Yale University, New Haven, Connecticut 06520, USA*

We derive a closed expression for the linear conductance through a quantum dot in the Coulomb-blockade regime in the presence of a constant exchange interaction. With this expression we calculate the temperature dependence of the conductance peak-height and peak-spacing statistics. Using a realistic value of the exchange interaction, we find significantly better agreement with experimental data as compared with the statistics obtained in the absence of an exchange interaction.

PACS numbers: 73.23.Hk, 05.45.Mt, 73.40.Gk, 73.63.Kv

The conductance through a quantum dot that is weakly coupled to leads displays sharp peaks as an applied gate voltage is varied. Each conductance peak describes the addition of one more electron into the dot, and between peaks the conductance is “blocked” by the Coulomb interaction. The statistics of both peak heights and peak spacings in dots for which the single-electron dynamics is chaotic have been intensively studied in recent years [1]. Some of the experimental observations, e.g. the peak-height distributions at low temperature [2, 3, 4], could be explained at least qualitatively by the constant-interaction (CI) model, in which the interaction is represented in the simple form of an electrostatic charging energy. Other measured observables, such as the peak-spacing distribution [5], have indicated that spin and residual interactions beyond the charging energy should be taken into account. A consistent theoretical approach that provides quantitative agreement with both the measured peak-height and peak-spacing statistics is still lacking.

Recently, a universal Hamiltonian was derived [6, 7] for a dot with a large Thouless conductance $g_T \sim \sqrt{N}$ (N is the number of electrons). An important contribution to the interaction part of this Hamiltonian is a constant exchange interaction in addition to the usual charging-energy term. The remaining interaction terms are suppressed at large g_T . Here we study the effect of the exchange interaction on the finite-temperature statistics of both peak heights and spacings. To this end, we derive a closed expression for the conductance in the presence of a constant exchange interaction (in the sequential-tunneling limit). This formula expresses the conductance in terms of quantities that characterize spinless non-interacting electrons. We then calculate the finite-temperature peak-height and peak-spacing statistics and find them both to be sensitive to the exchange interaction. Using an RPA estimate of the exchange interaction for the samples studied experimentally in Refs. [5, 8], we obtain very good agreement with the observed temperature dependence of the standard deviation of the peak spacing. We also explain most of the known discrepan-

cies between the experimental peak-height statistics [8] and the predictions of the CI model for $kT \lesssim 0.6 \Delta$ (Δ is the mean spacing between spin-degenerate levels).

The universal Hamiltonian of a quantum dot in the limit $g_T \rightarrow \infty$ is given by [6, 7]

$$\hat{H} = \sum_{\lambda\sigma} \epsilon_\lambda a_{\lambda\sigma}^\dagger a_{\lambda\sigma} + \frac{e^2}{2C} \hat{n}^2 - J_s \hat{\mathbf{S}}^2, \quad (1)$$

where ϵ_λ are spin-degenerate single-particle levels ($\sigma = \pm 1$ labels the spin). The second term in Eq. (1), where C is the dot’s capacitance and \hat{n} is the total-particle-number operator, accounts for the electrostatic energy of the dot. The third term, in which $\hat{\mathbf{S}}$ is the total-spin operator, describes a constant exchange interaction with strength J_s . The occupation-number operator $\hat{n}_\lambda = \hat{n}_{\lambda+} + \hat{n}_{\lambda-}$ of any single-particle orbital λ commutes with the total spin, $[\hat{n}_\lambda, \hat{\mathbf{S}}] = 0$, and the Hamiltonian \hat{H} is invariant under spin rotations. Thus the eigenstates of \hat{H} are characterized by their particle number N , the configuration of orbital occupation numbers $\mathbf{n} = \{n_\lambda\}$ ($n_\lambda = 0, 1$ or 2), the total spin S , and the spin projection $S_z = M$. We label the eigenstates as $|N\mathbf{n}\gamma SM\rangle$ where the quantum number γ distinguishes between states with the same total spin S and particle configuration \mathbf{n} . The eigenenergies are given by $\epsilon_{\mathbf{n}S}^{(N)} = \sum_\lambda \epsilon_\lambda n_\lambda + e^2 N^2 / 2C - J_s S(S+1)$.

In the limit of sequential tunneling (when a typical tunneling width is small compared with kT and Δ), the conductance can be calculated using a rate-equations approach. In Ref. [9], we developed such an approach in the presence of interactions and spin. In particular, an explicit solution exists when the orbital occupation numbers n_λ are good quantum numbers. Expressing the conductance G in a rescaled form $G = (e^2 \bar{\Gamma} / 8\hbar kT) g$ (where $\bar{\Gamma}$ is an average width of a level), we have, in the vicinity of the $N+1$ -st Coulomb-blockade peak

$$g = 4 \sum_{\substack{\lambda\mathbf{n}\gamma S \\ \mathbf{n}'\gamma'S'}} \tilde{P}_{\mathbf{n}S}^{(N)} f(\epsilon_{S'S}^\lambda) |([N+1]\mathbf{n}'\gamma'S' \| a_\lambda^\dagger \| N\mathbf{n}\gamma S)|^2 g_\lambda. \quad (2)$$

Here $g_\lambda = 2\bar{\Gamma}^{-1} \Gamma_\lambda^l \Gamma_\lambda^r / (\Gamma_\lambda^l + \Gamma_\lambda^r)$ are the single-particle level conductances, where $\Gamma_\lambda^{l,r}$ are the partial widths of

an electron in orbital λ to decay to the left or right lead. The equilibrium probability of the dot to be in the state $|N\mathbf{n}\gamma SM\rangle$ is $\tilde{P}_{\mathbf{n}S}^{(N)} = e^{-\beta(\epsilon_{\mathbf{n}S}^{(N)} - \tilde{\epsilon}_F N)}/Z$, where the partition function Z is a Boltzmann-weighted sum over all possible N - and $(N+1)$ -body states (no other particle numbers contribute because of the charging energy), and $\tilde{\epsilon}_F = e\zeta V_g + \epsilon_F$ is an effective Fermi energy (ϵ_F is the Fermi energy in the leads, V_g is the gate voltage and $\zeta = C_g/C$ with C_g the dot-gate capacitance). The Fermi-Dirac function $f(x) = (1 + e^{\beta x})^{-1}$ is evaluated at an electron energy (relative to the Fermi energy) $\epsilon_{S'S}^\lambda = \epsilon_{\mathbf{n}'S'}^{(N+1)} - \epsilon_{\mathbf{n}S}^{(N)} - \tilde{\epsilon}_F$ that conserves energy at the transition between states $|N\mathbf{n}\gamma SM\rangle$ and $|(N+1)\mathbf{n}'\gamma'S'M'\rangle$. The corresponding reduced matrix element ($[N+1]\mathbf{n}'\gamma'S'\|a_\lambda^\dagger\|N\mathbf{n}\gamma S$) enforces the selection rule $S' = |S \pm 1/2|$.

Eq. (2) can be rewritten in the form

$$g = \sum_{\lambda} (w_{\lambda}^{(0)} + w_{\lambda}^{(1)}) g_{\lambda}, \quad (3)$$

where the contributions with $n_{\lambda} = 0$ and $n_{\lambda} = 1$ are collected in $w_{\lambda}^{(0)}$ and $w_{\lambda}^{(1)}$, respectively. For the cases with $n_{\lambda} = 0$, the final $(N+1)$ -particle state is given by $|(N+1)\mathbf{n}'\gamma'S'M'\rangle = \sum_{M\sigma} (SM\frac{1}{2}\sigma|S'M')a_{\lambda\sigma}^\dagger|N\mathbf{n}\gamma SM\rangle$, where $(SM\frac{1}{2}\sigma|S'M')$ is a Clebsch-Gordon coefficient. When $n_{\lambda} = 1$ (and hence $n'_{\lambda} = 2$), the N -particle state can be similarly related to the $(N+1)$ -particle state by changing to a hole representation. This leads to the following reduced matrix elements,

$$(\mathbf{n}'\gamma'S'\|a_{\lambda}^\dagger\|N\mathbf{n}\gamma S) = (-)^{S-S'-\frac{1}{2}} \begin{cases} \sqrt{2S'+1} & \text{if } n_{\lambda}=0, \\ \sqrt{2S+1} & \text{if } n'_{\lambda}=2. \end{cases} \quad (4)$$

Using the relation $\tilde{P}_{\mathbf{n}S}^{(N)} f(\epsilon_{S'S}^\lambda) = \tilde{P}_{\mathbf{n}'S'}^{(N+1)} [1 - f(\epsilon_{S'S}^\lambda)]$, we get

$$w_{\lambda}^{(0)} = 4 \sum_S b_{\lambda,N,S} P_{N,S} \sum_{S'=S\pm 1/2} (2S'+1) f(\epsilon_{S'S}^\lambda), \quad (5a)$$

$$c_{\lambda,N,S} = \frac{\langle \tilde{n}_{\lambda} \rangle_{\frac{N}{2}+S} \langle \tilde{n}_{\lambda} \rangle_{\frac{N}{2}-S} e^{-\beta(\tilde{F}_{\frac{N}{2}+S} + \tilde{F}_{\frac{N}{2}-S})} - \langle \tilde{n}_{\lambda} \rangle_{\frac{N}{2}+S+1} \langle \tilde{n}_{\lambda} \rangle_{\frac{N}{2}-(S+1)} e^{-\beta(\tilde{F}_{\frac{N}{2}+S+1} + \tilde{F}_{\frac{N}{2}-(S+1)})}}{e^{-\beta(\tilde{F}_{\frac{N}{2}+S} + \tilde{F}_{\frac{N}{2}-S})} - e^{-\beta(\tilde{F}_{\frac{N}{2}+S+1} + \tilde{F}_{\frac{N}{2}-(S+1)})}} \quad (9)$$

where \tilde{n}_{λ} is the particle-number operator of a non-degenerate orbital λ . The function $b_{\lambda,N,S}$ from Eq. (5a) is expressed by replacing \tilde{n}_{λ} by $(1 - \tilde{n}_{\lambda})$ in Eq. (9). The complete expression for the conductance is then obtained from Eqs. (3), (5), (6), (8), (9) and the relation indicated in the previous sentence. Thus the dot's conductance in model (1) is determined in terms of the free energy \tilde{F}_q and single-particle occupation numbers $\langle \tilde{n}_{\lambda} \rangle_q$

$$w_{\lambda}^{(1)} = 4 \sum_{S'} c_{\lambda,N+1,S'} P_{N+1,S'} \sum_{S=S'\pm 1/2} (2S+1) [1 - f(\epsilon_{S'S}^\lambda)], \quad (5b)$$

where the quantities $b_{\lambda,N,S} = \frac{1}{2} \langle (\hat{n}_{\lambda} - 1)(\hat{n}_{\lambda} - 2) \rangle_{N,S}$ and $c_{\lambda,N,S} = \frac{1}{2} \langle \hat{n}_{\lambda}(\hat{n}_{\lambda} - 1) \rangle_{N,S}$ ensure that the sum is only over contributions with $n_{\lambda} = 0$ or 1, respectively. They are defined in terms of thermal expectation values at constant particle number N and spin S , i.e. $\langle \hat{X} \rangle_{N,S} = \text{Tr}_{N,S}[\hat{X} e^{-\beta \hat{H}}] / \text{Tr}_{N,S}[e^{-\beta \hat{H}}]$. The quantity $P_{N,S}$ is the probability to find the dot with N electrons and spin S ,

$$P_{N,S} = e^{-\beta[F_{N,S} + U_{N,S}]} / Z, \quad (6)$$

where $F_{N,S} = -\beta^{-1} \ln \text{Tr}_{N,S} e^{-\beta \sum_{\lambda\sigma} \epsilon_{\lambda} a_{\lambda\sigma}^\dagger a_{\lambda\sigma}}$ is the free energy of N non-interacting electrons with total spin S and $U_{N,S} = e^2 N^2 / 2C - J_s S(S+1) - \tilde{\epsilon}_F N$.

The spin-projected trace of a scalar observable can be calculated from traces at fixed spin projection M using $\text{Tr}_{N,S} \hat{X} = \text{Tr}_{N,M=S} \hat{X} - \text{Tr}_{N,M=S+1} \hat{X}$. For spin-1/2 particles, the projection on fixed particle number N and spin projection M is equivalent to projecting on a fixed number of spin-up and spin-down particles $n_{\pm} = N/2 \pm M$. Therefore,

$$\text{Tr}_{N,S} \hat{X} = \text{tr}_{\frac{N}{2}+S, \frac{N}{2}-S} \hat{X} - \text{tr}_{\frac{N}{2}+S+1, \frac{N}{2}-(S+1)} \hat{X}, \quad (7)$$

where the traces ‘‘tr’’ on the r.h.s. are evaluated at fixed n_+ and n_- . Using $\hat{X} = e^{-\beta \sum_{\lambda\sigma} \epsilon_{\lambda} a_{\lambda\sigma}^\dagger a_{\lambda\sigma}}$ in Eq. (7) we find that the free energy in Eq. (6) is given by

$$e^{-\beta F_{N,S}} = e^{-\beta(\tilde{F}_{\frac{N}{2}+S} + \tilde{F}_{\frac{N}{2}-S})} - e^{-\beta(\tilde{F}_{\frac{N}{2}+S+1} + \tilde{F}_{\frac{N}{2}-(S+1)})}. \quad (8)$$

The free energy \tilde{F}_q in Eq. (8) is defined for q spinless particles $e^{-\beta \tilde{F}_q} = \tilde{\text{tr}}_q e^{-\beta \sum_{\lambda} \epsilon_{\lambda} c_{\lambda}^\dagger c_{\lambda}}$ where c_{λ}^\dagger and c_{λ} create and annihilate spinless particles in non-degenerate levels with energies ϵ_{λ} . The quantity $c_{\lambda,N,S}$ from Eq. (5b) can now be expressed as

of q non-interacting spinless fermions. Both \tilde{F}_q and $\langle \tilde{n}_{\lambda} \rangle_q$ are familiar from earlier works in the framework of the CI model, and can be expressed in closed form using particle-number projection [see Eqs. (140) in Ref. [1]].

In chaotic dots, the single-particle Hamiltonian in (1) is described by random-matrix theory. We have studied the statistics of peak heights and spacings for both the orthogonal and unitary symmetries. The dimension

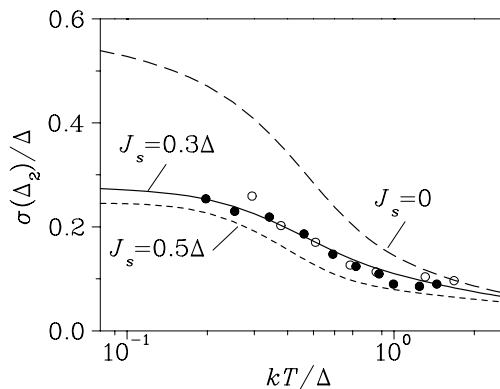


FIG. 1: The width $\sigma(\Delta_2)$ of the peak-spacing distribution for three different values of the exchange-interaction strength J_s . The symbols are the experimental data of Ref. [5].

of the configuration sum in Eq. (2) increases combinatorially with the number of single-particle orbitals and a direct use of (2) becomes impractical at higher temperatures. In contrast, the closed expression we derived greatly facilitates the calculation of the conductance for a rather large model system of 50 single-particle orbitals λ . We checked that our results are not affected by the finite size of the system up to temperatures of $kT \sim 3 \Delta$.

Theoretical calculations of the width $\sigma(\Delta_2)$ of the peak-spacing distribution, based on a spinless CI model [10], describe qualitatively the observed decrease of this quantity with increasing temperature [5]. However, a proper modeling of the peak-spacing distribution itself requires the inclusion of spin. When spin is included and in the absence of an exchange interaction, the calculated values of $\sigma(\Delta_2)$ (long-dashed line in Fig. 1) show a large discrepancy with the experimental values (symbols). Fig. 1 also shows $\sigma(\Delta_2)$ for non-zero values of J_s . For a gas constant of $r_s \sim 1.2$ (that corresponds to the samples used in the experiments), the RPA estimate is $J_s \approx 0.3 \Delta$ [11], and we find for this value a very good agreement with the measurements. The results for $J_s = 0.5 \Delta$ underestimate the experimental widths. We remark that at temperatures $kT \lesssim 0.4 \Delta$, the model (1) does not describe well the shape of the peak-spacing distribution, and it is necessary to include the fluctuating part of the universal Hamiltonian to explain the absence of bimodality [12, 13]. At higher temperatures, the bimodality is absent already in model (1) and the residual interaction has a negligible effect on the width.

Another measured quantity is the ratio between the standard deviation $\sigma(g_{\max})$ and the average \bar{g}_{\max} of the peak heights g_{\max} [8]. The experimental data for this ratio (symbols in Fig. 2) are seen to be suppressed in comparison with the results of model (1) without an exchange term (long-dashed line in the left panel of Fig. 2). Spin-orbit interaction was proposed as a mechanism for this suppression at low temperatures [14]. It was neces-

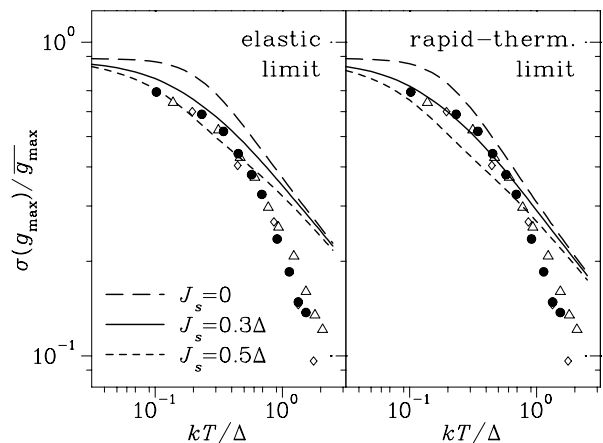


FIG. 2: The ratio $\sigma(g_{\max})/\bar{g}_{\max}$ between the standard deviation and the average value of the peak height versus temperature kT . The left (right) panel shows data in the case of the elastic (rapid-thermalization) limit for three different strengths of the exchange interaction $J_s = 0$ (long-dashed), 0.3Δ (solid), and 0.5Δ (short-dashed). The symbols are the experimental data of Ref. [8].

sary to assume a spin-orbit coupling that is sufficiently strong to completely decorrelate the spin-up and spin-down levels. However, spin-orbit effects are likely to be suppressed in the small dots used in the experiment. To determine whether an exchange interaction can explain the observed suppression of $\sigma(g_{\max})/\bar{g}_{\max}$, we calculated this ratio versus temperature kT for different strengths of the exchange interaction (see Fig. 2). In the elastic limit (left panel), a realistic exchange interaction of $J_s = 0.3 \Delta$ leads to closer agreement with the data. The remaining small discrepancy at temperatures $kT \lesssim 0.6 \Delta$ can probably be accounted for by adding a realistic weak spin-orbit interaction. It still remains to explain the discrepancy at higher temperatures, where inelastic scattering may play a role. The calculation of Ref. 15 showed that the suppression of $\sigma(g_{\max})/\bar{g}_{\max}$ due to inelastic scattering is small for $J_s = 0$. In the right panel of Fig. 2 we show results for the rapid-thermalization limit of strong inelastic scattering in the presence of an exchange interaction. While the agreement (for $J_s = 0.3 \Delta$) is now better at low temperatures, we do not expect inelastic scattering to be important at these temperatures. At higher temperatures, the rapid-thermalization limit does not describe the data, and it would be interesting to determine the effect of an additional weak spin-orbit term.

For $kT \ll \Delta$ and $J_s = 0$, the peak-height distribution $P(g_{\max})$ can be calculated analytically [2] and is shown for the unitary symmetry as a solid line in the left panel of Fig. 3 (compared to the case of spinless electrons, the peak heights are rescaled [1] by $8(\sqrt{2}-1)^2 \sim 1.37$). Also shown (histogram) is the peak-height distribution calculated at $kT = 0.01 \Delta$ and $J_s = 0.5 \Delta$. No significant

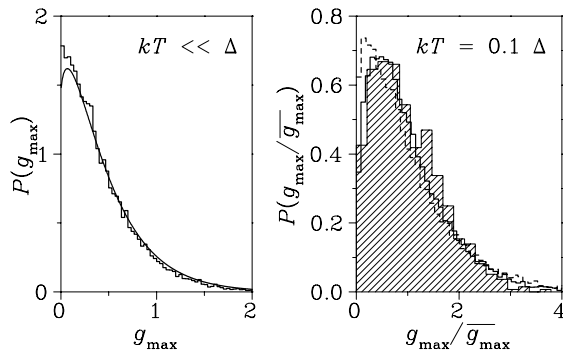


FIG. 3: Peak-height distributions. Left panel: The analytically known distribution $P(g_{\max})$ at $kT \ll \Delta$ and $J_s = 0$ (smooth curve) is compared with the corresponding distribution at $kT = 0.01 \Delta$ and $J_s = 0.5 \Delta$ (histogram). Right panel: Experimental data from Ref. [8] (gray-shaded histogram) at $kT = 0.1 \Delta$ are compared with the calculated distributions at $J_s = 0$ (dashed histogram) and $J_s = 0.3 \Delta$ (solid histogram).

effect due to exchange is observed except for a small enhancement of the probability at small peak heights.

At finite temperature, the exchange interaction has a stronger effect on the peak-height distribution. The right panel of Fig. 3 compares the histogram (gray shaded) of the experimental data for $P(g_{\max}/\bar{g}_{\max})$ at $kT = 0.1 \Delta$ with the calculated histograms for the cases of no exchange ($J_s = 0$) and $J_s = 0.3 \Delta$. This latter realistic value of the exchange interaction explains the observed suppression of the probability at small peak heights.

The weak-localization effect in the average peak height attracted recent attention both in experiment and theory [15, 16, 17, 18]. Its suppression at higher temperatures was suggested as a signature of inelastic scattering in the dot. The effect is quantified by the parameter $\alpha = 1 - (\bar{g}_{\max}^{\text{GOE}}/\bar{g}_{\max}^{\text{GUE}})$. In the rapid-thermalization limit, α decreases rapidly with increasing temperature from its value of 0.25 at $kT \ll \Delta$ [17]. In contrast, if inelastic scattering is negligible, α was expected to be temperature independent. However, calculations for $J_s = 0$ showed a slight suppression of the elastic α around $kT \sim 0.25 \Delta$ [15, 18]. This was understood by the fact that close lying levels and hence higher conductances are more likely for the orthogonal symmetry. The effect of the exchange interaction on α is shown in Fig. 4. We find that the dip in α around $kT \sim 0.25 \Delta$ is flattened out and in the small-temperature limit α becomes larger than 0.25. While α is seen to be sensitive to the exchange interaction at low temperatures, the experimental uncertainties of Ref. [16] are too large to observe this effect. In the rapid-thermalization limit, α is insensitive to J_s .

In conclusion, we have derived a closed expression for the conductance in the presence of spin and exchange interaction. Using this formula we studied the dependence of the peak height and spacing statistics on the exchange interaction and found a significantly better quantitative

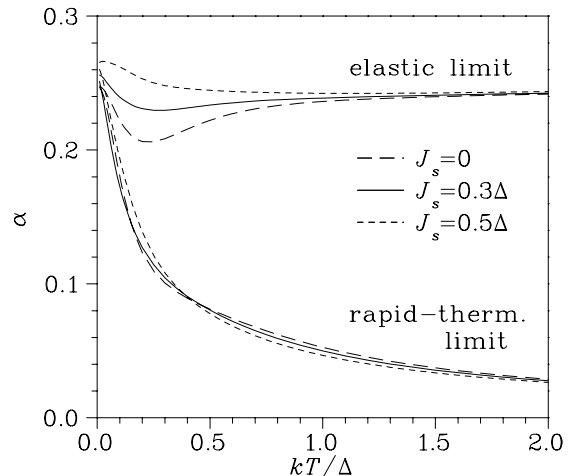


FIG. 4: The weak-localization parameter α versus temperature kT in the elastic and rapid-thermalization limit for three different values of the exchange-interaction strength J_s .

agreement with experiment than in the absence of an exchange interaction.

This work was supported in part by the U.S. DOE grant No. DE-FG-0291-ER-40608. We thank C. M. Marcus for helpful discussions.

-
- [1] Y. Alhassid, Rev. Mod. Phys. **72**, 895 (2000).
 - [2] R. A. Jalabert, A. D. Stone, and Y. Alhassid, Phys. Rev. Lett. **68**, 3468 (1992).
 - [3] A. M. Chang *et al.*, Phys. Rev. Lett. **76**, 1695 (1996).
 - [4] J. A. Folk *et al.*, Phys. Rev. Lett. **76**, 1699 (1996).
 - [5] S. R. Patel *et al.*, Phys. Rev. Lett. **80**, 4522 (1998).
 - [6] I. L. Kurland, I. L. Aleiner, and B. L. Altshuler, Phys. Rev. B **62**, 14886 (2000).
 - [7] I. L. Aleiner, P. W. Brouwer, and L. I. Glazman, Phys. Rep. **358**, 309 (2002).
 - [8] S. R. Patel *et al.*, Phys. Rev. Lett. **81**, 5900 (1998).
 - [9] Y. Alhassid, T. Rupp, A. Kaminski, and L. I. Glazman, arXiv:cond-mat/0212072.
 - [10] Y. Alhassid and S. Malhotra, Phys. Rev. B **60**, R16315 (1999).
 - [11] Y. Oreg *et al.*, in *Nano-Physics and Bio-Electronics: a New Odyssey*, eds. T. Chakraborty, F. Peeters and U. Sivan (Elsevier, 2002).
 - [12] G. Usaj and H. U. Baranger, Phys. Rev. B **64**, 201319R (2001); arXiv:cond-mat/0203074.
 - [13] Y. Alhassid and S. Malhotra, arXiv:cond-mat/0202453.
 - [14] K. Held, E. Eisenberg, and B. L. Altshuler, arXiv:cond-mat/0208177.
 - [15] T. Rupp, Y. Alhassid, and S. Malhotra, Phys. Rev. B **65**, 193304 (2002).
 - [16] J. A. Folk, C. M. Marcus, and J. S. Harris, Jr., Phys. Rev. Lett. **87**, 206802 (2001).
 - [17] C. W. J. Beenakker, H. Schomerus, and P. G. Silvestrov, Phys. Rev. B **64**, 033307 (2001).
 - [18] E. Eisenberg, K. Held, and B. L. Altshuler, Phys. Rev. Lett. **88**, 136801 (2002).